Hindawi
Advances in Civil Engineering
Volume 2024, Article ID 4830026, 15 pages
https://doi.org/10.1155/2024/4830026

Research Article

Experimental Investigation on Shear Strength and Microstructure of Chemically Treated Sisal Fiber-Reinforced Concrete

Abadi Haftu Kahsay [1] **and Belachew Asteray Demiss** [1,2]

[1]*College of Architecture and Civil Engineering, Department of Civil Engineering, Addis Ababa Science and Technology University, Addis Ababa, Ethiopia*
[2]*Department of Civil Engineering, Construction Quality and Technology Center of Excellence, Addis Ababa Science and Technology University, Addis Ababa, Ethiopia*

Correspondence should be addressed to Abadi Haftu Kahsay; haftuabadii@gmail.com

Received 20 December 2023; Revised 15 February 2024; Accepted 24 April 2024; Published 17 May 2024

Academic Editor: Liborio Cavaleri

The incorporation of sisal fiber into the concrete matrix reduces waste disposal, which has negative environmental impacts. The aim of this study was to perform an experimental investigation on shear strength and microstructure of chemically treated sisal fiber-reinforced concrete (SFRC). In order to accomplish the aim of the study, physical, shear, and mechanical properties of concrete reinforced with chemically treated sisal fiber have been performed. 0.50%, 1.00%, 1.25%, 1.50%, 1.75%, and 2.00% of sodium hydroxide (NaOH) and sulfuric acid (H_2SO_4) treated sisal fiber were used as an addition to the dry weight average with the help of the American Concrete Institute (ACI) mix design procedure. After the 7th and 28th days of curing, shear strength according to the ASTM D5379M standard and the mechanical properties of concrete have been conducted. For microstructural properties, scanning electron microscopy (SEM) and X-ray diffraction (XRD) were conducted after the concrete was cured for 28 days. Forty-six percent and 20% compressive strength enhancement at the 7th and 28th days of curing was compared to the control mix. Twenty-seven percent enhancement was recorded in the split tensile strength of 1.5% SFRC as compared to the control mix at 28 curing days. A shear strength of 1.5% SFRC was improved by 95% at the 7th curing days and 28% at the 28th curing days as compared to the control mix. As compared to conventional concrete, SFRC shows a denser microstructure. In addition to this, portlandite, quartz, calcium aluminum silicate, and C—S—H crystal are the available phases in the concrete matrix.

1. Introduction

Even if it is a widely used construction material, concrete is brittle in nature [1, 2]. Because of its demand growth throughout the world, concrete increases environmental burden [3]. Naturally, concrete has high capacity to bear load [4]. However, it possesses low shear resistance, low tensile strength, little resistance to cracking, and low ductility [5]. The low tensile strength and weak shear resistance of concrete are due to the propagation of microcracks [6–8]. The microcracks in concrete develop due to drying shrinkage even before loading [9, 10]. Over this cracked material, when a structural load is applied, the microcracks tend to propagate and open up due to stress, and additional cracks are formed. This crack propagation is the consequence of inelastic deformation in concrete [11]. From the study performed by Palanisamy et al. [3], advancements in material technology have led to the production of modern materials and environmental and energy conservation, necessitating the use of creative design processes in the current environmental design thinking.

The formation of cracking is not only due to dry shrinkage of concrete but also due to corrosion of the reinforcement [12]. Chloride ion ingresses and carbon dioxide reacted with the cement paste due to poor-quality concrete. Corrosion can be reduced by using high-quality concrete. High-quality concrete is produced from fiber reinforcement. For preservation

and conservation of cultural heritage buildings, repairing, strengthening, and retrofitting using fibers are preferable. These strengthening and retrofitting improve structural bearing of the building [13]. The use of fibers in concrete matrix is due to tensile behavior, the shear bond properties, and the compatibility of the fibers [14].

To strengthen tensile strength, shear strength, and the ductility of concrete, synthetic and natural fibers have been tried as reinforcements [15]. Synthetic fibers have better strength as compared to natural fibers [16]. However, the production of synthetic fiber is not environmentally friendly. It consumes more energy, and its process and production have a negative environmental impact. The disposal and management of waste materials are facing significant challenges, leading to significant pollution concerns [17]. The use of waste materials in concrete production does have dual benefit. The first one is reducing waste disposal and protecting environmental pollution. As stated by Velusamy et al. [18], using waste materials for ecofriendly concrete production is the solution to minimize waste disposal. The other important thing is the production of compatible and sustainable concrete structure with low cost and low energy using locally available ecofriendly materials [19]. According to the study made by Arunkumar et al. [20], the utilization of locally available materials can reduce costs and environmental impacts.

Due to their local availability (an environmental friend) and low cost of production, natural fibers have been preferred to synthetic fibers [21]. The use of natural fibers has a positive impact on the environment by minimizing waste disposal in the environment [22]. If utilized properly, natural fibers have comparable strength to synthetic fibers. The use of natural fiber in concrete matrix does not require specialized workers as synthetic fibers do. It can be done with only a small number of trained workers [11].

Due to their light weight, economical cost, greater specific strength and modulus, and no health risk, natural fibers are promising reinforcements for the use in concrete and are easily procured in many countries [23]. Natural fiber like sisal fiber and coir is nowadays used for strengthening and repairing of concrete structures. Flooring and roofing components, pipes, manhole covers and frames, and precast thin-wall elements are among the predominant uses of natural fibers these days [24]. Natural fibers like sisal fiber evaluated from the ecological aspect are more preferable than synthetic fibers. Because natural fibers like sisal fiber are a waste and inexpensive, they are more preferable to synthetic fibers [10]. Because of their availability, low cost, and low consumption of energy, sisal fiber is preferable to natural fibers like jute fiber, coir fiber, and bamboo fiber [25].

Sisal fiber is one of the most commonly used natural fibers in concrete production [26]. It is obtained from the leaves of the sisal plant (scientifically called *Agave sisalana*) [27]. The sisal plant is one of the most extensively cultivated fibers throughout the world and in Ethiopia. The bonding between the fiber and concrete matrix, the structure of the fiber reinforced, the cementitious material used, and the aspect ratio of the fiber are the most important properties affecting the performance of the sisal fiber-reinforced matrix [28]. Improved microcracking, tensile strength, and shear resistance are the major roles of sisal fiber [29].

Manually extracted sisal fiber incorporates impurities like hemicellulose, lignin, and other residuals. Using sisal fiber, with its impurities, reduces the bonding matrix of the concrete material. To enhance this, chemical treatment of sisal fiber is a solution. According to Mithun et al. [30], alkaline treatment partially removes lignin and hemicellulose [27]. The aim of the researcher is therefore to investigate the shear strength and microstructure of concrete reinforced with sodium hydroxide and sulfuric acid treated sisal fiber. Sodium hydroxide (alkaline) is used to remove the impurities in the sisal fiber [31]. However, alkaline treatment (1) does not completely remove the impurities and (2) does have a negative impact on the hydration reaction of the concrete matrix due to the Na^+ and OH^- when reacted with water, sulfuric acid treatment was supplied. The sulfuric acid treatment performs double activity: removing excess impurities and neutralizing the sisal fiber by reacting with sodium hydroxide. The aim and scope of the study are, hence, investigating shear strength and the microstructural and mechanical properties of concrete reinforced with chemically treated sisal fiber. In order to achieve the experimental investigation of the shear strength and microstructural properties of SFRC, physical and mechanical tests were conducted in AASTU and ASTU laboratories.

2. Materials and Methodology

In this section, the materials, including their source, and the methods used in the experimental investigation are discussed. The method of the study describes the process of sisal fiber extraction, material preparation, and an experimental program.

2.1. Materials. The materials used in this study are cement, fine aggregate, course aggregate, water, and sisal fiber.

2.1.1. Cement. Cement is a binding agent used in concrete production that adheres the other concrete constituents together. Ordinary portland cement (OPC) is designed for general construction work throughout the world. A locally produced 42.5 grade of Dangote OPC denoted as 42.5R is used in this study, where R indicates rapid early strength. As referred to in the factory products, the cement grade is produced according to the standard of the American Society for Testing and Materials (ASTM) C150.

2.1.2. Fine Aggregate. Fine aggregate is an inert material used for concrete production. It is the most consumed material next to coarse aggregate [32]. The fine aggregate used in this study was a natural river sand that passes through IS sieve 4.75 mm sizes as per ASTM standards. The physical characterization of fine modulus based on ASTM C33-03, specific gravity and water absorption based on ASTM C128-01, moisture content based on ASTM C566-97, and silt content based on ASTM C117-04, was conducted in the laboratory of Addis Ababa Science and Technology University (AASTU).

Figure 1: Physical characterization of fine and course aggregates.

2.1.3. Coarse Aggregate. Coarse aggregate is the most commonly used inert ingredient in concrete production [33]. In this research, for coarse aggregate, basaltic crushed rock based on the standards of ASTM produced in Addis Ababa, Ethiopia, was used. Sieve analysis tests based on ASTM C136, specific gravity tests and water absorption tests based on ASTM C128, and moisture content tests based on ASTM C566 were conducted in the AASTU laboratory. The physical characterization of fine and coarse aggregate is indicated in Figure 1.

2.1.4. Water. Water is the reaction catalyst in concrete. Impurities in water (silt, salt, acid, and other chemicals) can adversely affect the strength and quality of concrete by affecting the hydration reaction that takes place in the concrete matrix [34]. Therefore, in this study, a distilled water produced in the AASTU biological laboratory is used.

2.1.5. Sisal Fiber, Its Extraction, and Treatment. Sisal plant is available in most parts of Ethiopia [29, 35]. Sisal fiber sourced from different areas has different properties. The sisal fiber for this research was obtained from the compound of Addis Ababa Science and Technology University. After being manually extracted from the sisal plant, the sisal fiber was washed with drinking water two times and with tap water one time to remove the debris and impurities and gain its strength for resisting loads. Then it was treated with 2% NaOH for 4 hr in a contained vacuum. The vacuumed treatment is for reducing environmental contamination and moisture absorption of NaOH from the air [36]. Then the alkaline treated sisal fiber was washed with clean water and dried for 2 hr. To sisal fiber (Cell-OH), NaOH is the best feasible treatment. The alkaline removes the hydrogen bonding and then increases the roughness of the surface of the fiber. All impurities in sisal fiber do not dissolve and are treated with NaOH. To completely remove the impurities, it is necessary to treat them with acid [37]. In this study, 1 ml concentration of sulfuric acid was used to re-treat sisal fiber. The sisal fiber extraction process is shown in Figure 2.

Sisal fiber is a natural fiber extracted from sisal plant (*A. sisalana*). To remove impurities in the sisal fiber, the fiber was treated with 2% NaOH for 4 hr in a closed environment to remove hemicellulose and lignin impurities. The environment was closed by covering it with plastic. After this, the sisal fiber was washed again with 1 ml concentration of sulfuric acid by soaking the sisal fiber for 2 hr to remove some excess sodium hydroxide and some of the alkaline undissolved impurities. The acid treatment used has three benefits in this study. The first one is to remove excess sodium hydroxide from the fiber. The second one is to remove some excess impurities that did not dissolve by sodium hydroxide treatment. The third and most important is to improve the water absorption capacity of sisal fiber, which affects the durability of concrete. After such treatments, the hydrophilic (absorbs water) nature of sisal fiber was changed to hydrophobic (does not absorb water). Finally, the sisal fiber was washed with water again to remove excess sulfuric acid from the fiber [27, 38]. The size of sisal fiber used was prepared based on the standard of ASTM D 3822-07 [39].

2.2. Mix Design. The objective of concrete mix design (mixing proportion) is to determine the most economical and practical combination of readily available materials that will satisfy the performance requirement under a particular condition of use. The mix proportioning was carried out by following the ACI mix proportion process for this experimental work. The proportions of the concrete mix are typically expressed on the basis of the ingredients' mass per unit volume. The proportioning of concrete by the method of absolute volume requires the measurement of the volume of each ingredient and its contribution to the concrete output of 1 m^3. Volumes are subsequently converted to design weights. These conversions to weights are accomplished by taking the known volumes of ingredients and multiplying by the specific gravities of ingredients and again multiplying by the density of water.

In this specific research mix design of sisal fibers, reinforced concrete with determined ratios of cement, sand, water, coarse aggregate, and sisal fiber was proportioned for C25 concrete grade. The concrete mix design has been carried out for various proportions as per ACI 318 standard and arrived at final mix proportion.

For the production of SFRC, seven test trials have been mixed, with an addition of 0% (control mix-c), 0.5% (P1),

Figure 2: Sisal fiber extraction process: (a) sisal plant, (b) cutting sisal leaf, (c) manual extraction of sisal fiber, (d) chemical treatment of sisal fiber, (e) washing chemically treated sisal fiber, and (f) cutting sisal fiber in to useable fiber size (5 mm).

Table 1: Mix ratio of SFRC.

Materials (m^3)	Cement	Sand	Coarse aggregate	Water
in kg.	359.44	686.94	1,188.25	193.07

1.00% (P2), 1.25% (P3), 1.5% (P4), 1.75% (P5), and 2.00% (P6) mix of sisal fiber as a percentage of dry weight concrete. The mixing procedure was based on ACI-318. For each mix, three trial tests were prepared for the 7th and 28th days of curing, and the average of the three trials was used as the final result. The mix ratio for concrete reinforced with chemically treated sisal fiber is indicated in Table 1.

2.3. Laboratory Tests. Physical and mechanical tests were conducted in the laboratory. Sieve analysis, moisture content, specific gravity, and water absorption of fine and coarse aggregates are among the physical properties studied. Compressive strength, shear strength, and split tensile strength are the mechanical properties of concrete performed in the laboratory for this study. A laboratory test for concrete work is indicated in Figure 3.

2.3.1. Laboratory Tests for Physical Properties. In this specific research, basaltic crushed rock aggregates having nominal maximum size of 25 mm were made use of throughout the test in order to keep gradation in the range specified on ASTM standard. Physical property tests like gradation, specific gravity, water absorption, moisture content, and unit weight of the aggregates were conducted. For fine aggregate, silt content, gradation, specific gravity, water absorption, and moisture content of the fine aggregates were conducted.

A water absorption test is used to determine how much water the fine and coarse aggregates absorb during mixing. This helps determine the amount of water to be used in concrete production. Sieve analysis was made to identify the gradation of different sizes and to know the fine modulus of aggregate. Moreover, a specific gravity test was conducted to identify the quality and strength of the aggregate used. Specific gravity is the ratio of solid wood density to water

(a) (b) (c)

(d) (e) (f)

Figure 3: (a) Formwork oiling, (b) mixing, (c) molding, (d) formwork removing, (e) curing, and (f) testing.

Figure 4: Slump test (workability).

density at the same temperature, determined using green volume, ovendry volume, or intermediate volumes [20]. All physical tests of the research were conducted in the laboratory of AASTU.

To investigate the consistency of the concrete mix, a slump test was performed for each batch. It is a measure of the workability of fresh concrete [40]. The workability of the fresh concrete is a key attribute that determines the quality of a potential hardened form of the concrete. The term workability describes the capability of fresh material to be well handled and flow into the formwork or around the particular area of the structure where it is required. The slump test was performed following the procedures of ASTM C 143 "slump of hydraulic cement concrete." After the ingredients are mixed, the fresh concrete is immediately tested for slump using a cylindrical cone with a height of 300 mm and a diameter of 100 mm, as shown in Figure 4.

2.3.2. Laboratory Tests for Mechanical Properties. The experimental program is aimed to investigate the mechanical behavior, shear strength, and microstructure of concrete reinforced with chemically treated sisal fiber. To evaluate the effect of sisal fiber on the concrete strength, a number of tests are conducted. Due to the different behaviors observed for SFRC composites, research studies were carried out to identify the main parameters that characterize the

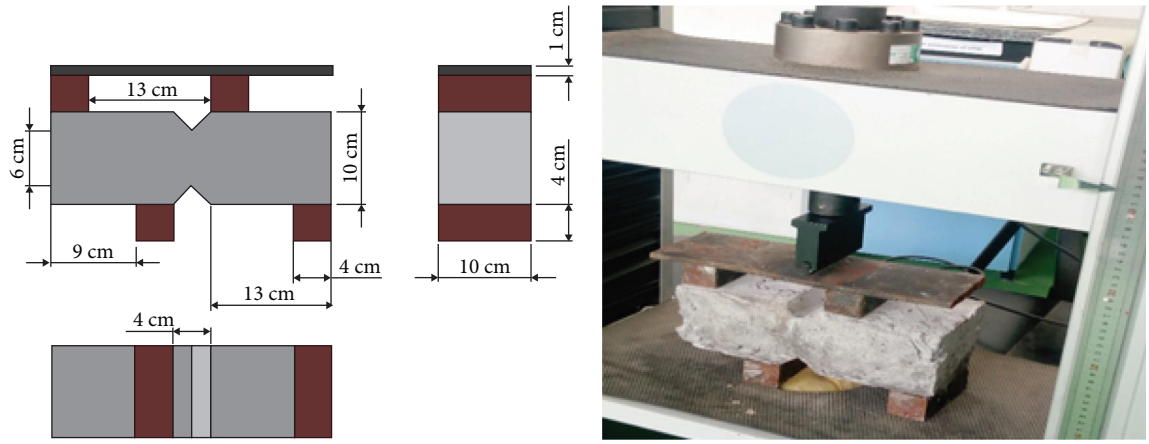

Figure 5: Shear strength test setup.

mechanical response of these materials due to sisal fiber treated with chemical.

(1) Compressive Strength Test. According to the British Standards Institute, the compressive strength of the test specimens of hardened concrete is determined using cube, cylinder, or core meeting the specified requirements, whereby the specimens are loaded to failure in a compression testing machine [41]. A compressive strength test determines a material's resistance to compression loads. In this study, a compressive strength test was done according to BS 1881-116 standards. Cubes of 150 mm were cast and cured in a soaking tank for 7 and 28 days for compressive strength tests. After curing, the cub samples were tested on a universal testing machine of 4,000 kN capacity with 2.5 K/s pace rates.

(2) Split Tensile Strength Test. A technique for assessing the tensile strength of concrete is the fracturing tensile strength test on concrete cylinders. The concrete is very poor in tension due to its brittle nature and is not designed to withstand direct tension. The concrete develops cracks when subjected to tensile forces. Thus, it is important to measure the tensile strength of concrete by finding the load at which the concrete members will crack. Split tensile strength of cylindrical samples having 30 cm height and 15 cm diameter were tested after 7 and 28 days of curing in accordance with ASTM C496 standard testing methods. Split tensile strength is the ability of a material to resist or withstand tensile force.

(3) Shear Strength Tests. Shear strength is defined as the ability of a material to resist two equal and oppositely directed forces whose lines of action are in planes very close together. A shear strength test was done based on ASTM D5379M Iosipescu test setup standards. One hundred millimeter by 100 mm × 300 mm size V-notched beam concrete specimens were prepared for the test. According to the Iosipescu shear test setup, load is applied nonsymmetrically through a five-point loading system. A pure shear section is maintained, and there is no bending (zero bending) at the center of the samples in the testing process. The shear strength test setup is shown in Figure 5.

2.3.3. Laboratory Tests for Microstructure.

(1) Scanning Electron Microscopy (SEM). This test was made to investigate the interfacial image of the concrete samples. A 1 cm × 1 cm sample was prepared immediately after a compressive strength test of a sample cured for 28 days. This 1 cm × 1 cm-sized concrete sample was tested in the material laboratory of Adama Science and Technology University (ASTU) at Adama, Oromia, Ethiopia. SEM samples were tested using a benchtop SEM machine and scanned through 600x, 1,100x, and 2,000x resolutions.

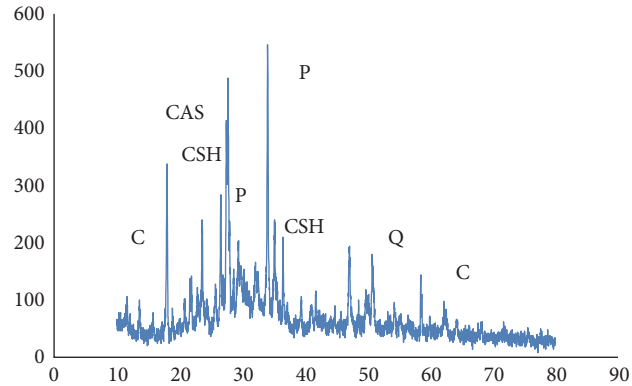

Figure 6: XRD result for control mix at 2θ. P, Portlandite; CAS, Calcium aluminium silicate; Q, Quartz; C, Calcium; CSH, Calcium silicate hydrate.

(2) X-ray Diffraction (XRD). An XRD test was also conducted at the material laboratory of ASTU to investigate the composition of the SFRC matrix. Immediately, after a compressive strength test was performed on 28-day cured specimens, powder was prepared by crushing and grinding. Powdered samples from C, P1, P2, P3, and P4 were placed on the XRD testing machine of the XRD-700 model X-ray diffractometer at an angular position of 2θ, as shown in Figures 6–10.

3. Results and Discussion

In this section, sieve analysis, moisture content, silt content, water absorption, and specific gravity as physical characterization and shear strength, compressive strength, split tensile strength, and bond strength as mechanical properties have been discussed.

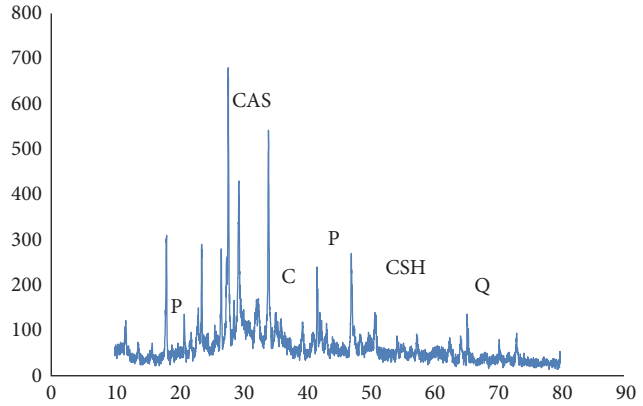

Figure 7: XRD result for P1 at 2θ. P, Portlandite; CAS, Calcium aluminium silicate; Q, Quartz; C, Calcium; CSH, Calcium silicate hydrate.

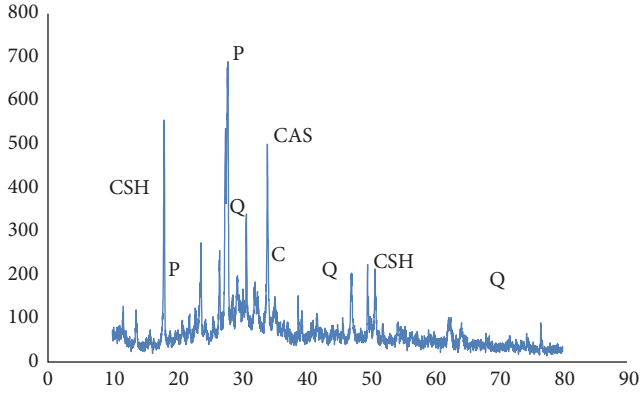

Figure 8: XRD result for P2 at 2θ. P, Portlandite; CAS, Calcium aluminium silicate; Q, Quartz; C, Calcium; CSH, Calcium silicate hydrate.

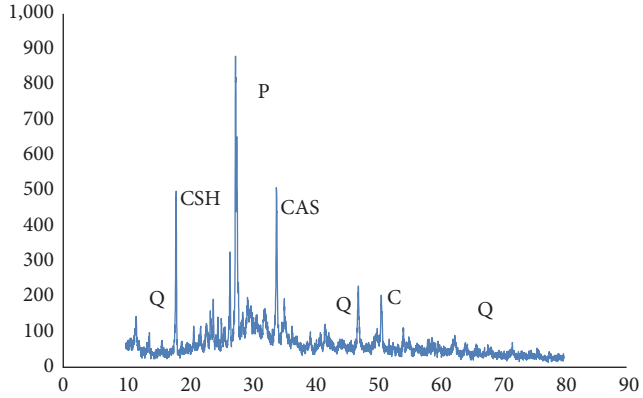

Figure 9: XRD result for P3 at 2θ. P, Portlandite; CAS, Calcium aluminium silicate; Q, Quartz; C, Calcium; CSH, Calcium silicate hydrate.

3.1. Results of Physical Tests

3.1.1. Sieve Analysis. Sieve analysis is undertaken to check the confirmation of the grading of the aggregate with ASTM C33-03. According to ASTMC33-03, the passing fine aggregate shall not exceed 45%. In line with this, ASTM specifies that the fine modulus range of fine aggregate is between 2.3 and 3.1. Out of this range, the fine aggregate to be used in the concrete matrix affects the workability, strength, and durability of the concrete. The cumulative passing of the fine aggregate is within the permissible range of ASTM. The fine modulus of the fine aggregate used in this study, as shown in Table 2, is within the permissible limit of ASTM C33-03. The fine modulus of coarse aggregate is shown in Table 2:

$$\text{Fineness modulus (FM)} = \frac{\sum \text{Cumulative coarser}}{100}, \quad (1)$$

$$\text{FM} = \frac{282}{100} = 2.87. \quad (2)$$

3.1.2. Silt Content. According to ASTM standards, a fine aggregate less than the No. 200 (75 μm) sieve is considered silt. The availability of excess silt content in fine aggregate reduces the quality of cement paste. This affects the strength and bonding ability of concrete. After washing and drying the fine aggregate, three trial silt content tests were conducted. Accordingly, 3.90%, 3.19%, and 3.72% were the results of the trial. From this, the silt content is taken as an

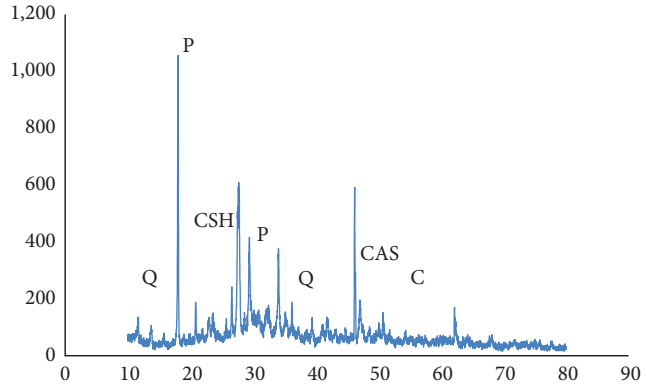

Figure 10: XRD result for P4 at 2θ. P, Portlandite; CAS, Calcium aluminium silicate; Q, Quartz; C, Calcium; CSH, Calcium silicate hydrate.

Table 2: Physical tests on fine and coarse aggregates.

Description	Test results	
Aggregate type	Fine aggregate	Course aggregate
Silt content	3.61%	—
Nominal aggregate size	—	25 mm
Fines modulus	2.88	3.0
Water absorption (%)	1.21	1.63
Moisture content (%)	2.32	1.75
Bulk specific gravity	2.14	2.81
Apparent specific gravity	2.21	2.95
Bulk SSD specific gravity	—	2.86

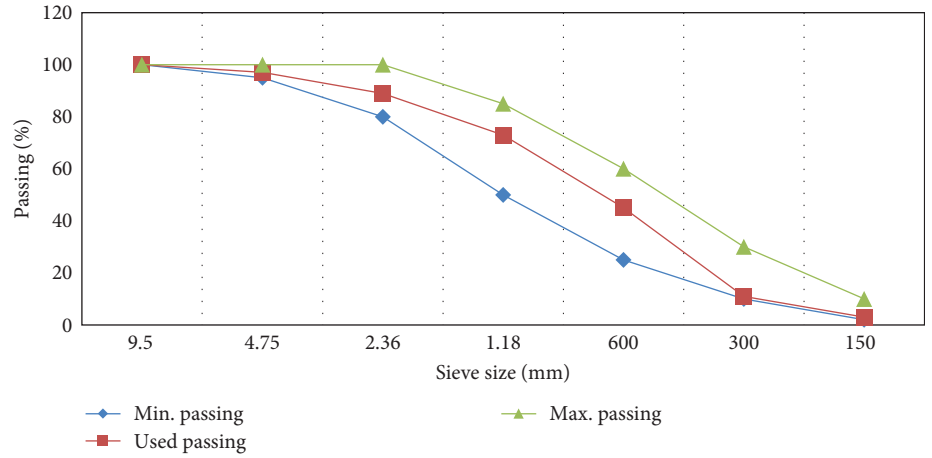

Figure 11: Sieve analysis of fine aggregate.

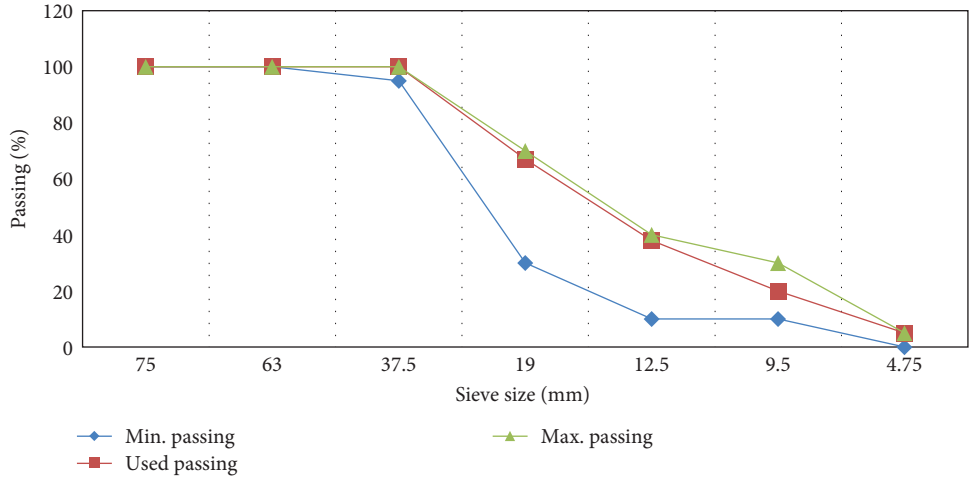

Figure 12: Sieve analysis of coarse aggregate.

average of the three trials, which is 3.61%. The permissible limit of silt content, according to ASTM C117-04, is 6%. Since 3.61% is less than 6%, the silt content of the fine aggregate is acceptable. This is also acceptable according to the Ethiopian Compulsory Standard's (ECS), in which permissible content is 6%. The gradation results of fine and coarse aggregate are indicated in Figures 11 and 12, respectively.

Moisture content is the measure of the water requirement in concrete mix. According to the moisture content of the aggregate, water consumption in concrete is adjusted. The moisture content of the fine aggregate and coarse aggregate used in this study was 2.32% and 1.75%, respectively. The water content to be used in the concrete matrix has been adjusted according to the ACI mix design procedure. Moisture content determination is in accordance with ASTM C566-97.

Its workability is known to be the ease with which fresh concrete can be shaped, molded, and compacted without segregation. It is a freshly mixed concrete property that shows the amount of internal work required to overcome the internal tension between the concrete's individual constituents. There was a decrease in slump height as addition of sisal fiber increases as compared to standard concrete. This decrease in concrete workability was due to the presence of fibers in the mix that tend to lump, ball, and absorb some of the free water required for lubrication and paste formation. There is also the occurrence of poor adhesion between fibers and the matrix as more fiber is added (greater than 1.5% sisal fiber). Therefore, the mix required more efforts to compact. The sieve analysis of fine aggregate is shown in Table 3.

3.2. Results of Mechanical Tests. The compression-loaded plain concrete specimens experienced a highly unstable failure mode, while the sisal fiber-reinforced concrete displayed a more robust nature. It can be checked from the outcome that the impact on the strength level of the sisal fiber has a deleterious effect. For compressive strength tests, six trial mixes for each batch were cured (three samples for a 7-day compressive strength test and three samples for a 28-day compressive strength test). The 7th and 28th days of compressive strength test results for C, P1, P2, P3, P4, P5, and P6 are 19.89, 22.86, 24.27, 26.28, 28.96, 27.25, 35.85, and 26.04 MPa for the 7th day and 31.19, 33.13, 33.8, 36.72, 37.37, 35.85, and 29.82 for the 28th day, respectively. The compressive strength of SFRC at the 7 and 28 days shows an enhancement up to a

Table 3: Sieve analysis and fine modulus of fine aggregate.

No.	Sieve size	Weight retained (kg)	Retained (%)	Cumulative retained (%)	Cumulative passing (%)	ES C.D3.201 cumulative passing (%)
1	9.5 mm	0	0	0	100	100
2	4.75 mm	15	3.06	3.06	9.94	95–100
3	2.36 mm	40	8.16	11.22	88.78	80–100
4	1.18 mm	80	16.33	27.55	72.45	50–85
5	600 μm	140	28.57	56.12	43.88	25–60
6	300 μm	170	34.69	90.82	9.18	5%−30
7	150 μm	45	9	99.82	0.18	0%−10
8	Pan	—	—	—	—	—
	Total	490	—	288.6	—	—

certain limit (P4 = 1.5% with the addition of sodium hydroxide and sulfuric acid treated sisal fiber). Using a 0.5% addition of chemically treated sisal fiber, a 15% increase is shown on the 7th day and a 6% increase on the 28th day from the control mix. When 1.00% chemically treated sisal fiber is added, it has 24.27 MPa at 7 days, which is 22% higher than C. In the same batch, the compressive strength at the 28th day was recorded to be 33.8 MPa, which is 8% higher than C.

The compressive strength of 0.5% addition, as compared to the expected compressive strength in the mix design, shows a 2.4% enhancement. Eighteen percent and 20% increments were shown if 1.25% and 1.50% sodium hydroxide and sulfuric acid treated sisal fiber were used on the 28th day of curing, respectively. This is 11.3% and 13.2% higher than the expected mean compressive strength stated on the mix design. In the same batch, the compressive strength shows an enhancement of 32% and 46% as compared to the control mix C. As shown in Figure 13, at P5 (1.75%) and P6 (2.00%), the compressive strength tends to decrease both at the 7th and 28th days of curing. The mean compressive strength of SFRC for the 7th and 28th curing days is labeled in Figure 13.

According to previous works on fiber-reinforced concrete (FRC), enhancements have been recorded in compressive strength due to fiber addition. According to the study by Shah et al. [42], the compressive strength of concrete with the addition of treated sisal fiber shows enhancement because of the compatibility formed in the surface of sisal fiber and concrete matrix. On the other side, the compressive strength of concrete tends to decrease when the percentage of raw sisal fiber is increased. In line with this study, sisal fibers enhance the mechanical strength of concrete due to the stored water available, which is released over time and causes strength development [43]. By using 0.5%, 1%, and 1.5% proportions of sisal fiber, 4.53%, 16.56%, and 29.69% enhanced compressive strength properties were observed as compared to the control mix (0% fiber), while a decrease of 38.83% was recorded when 2% of sisal fiber was used relative to the control mix based on the compressive test of the 7th day.

At the 28th day of curing, the compressive strength of sisal fiber improves by 5.17%, 12.5%, and 31.03% and decreases by 14.22% as 0.5, 1%, 1.5%, and 2% of sisal fiber addition are used, respectively [44]. On the same area, using sisal fiber and M-sand in 0.5% and 1% proportions, the compressive strength was 19.4 and 21.3 MPa, which is a 13% and 24% enhancement of the compressive strength, and at 1.5% composition, the compressive strength was 20.81, which is 2% reduced from the compressive strength attained using the 1% composition [45]. Using 0.5% and 1% sisal fiber composition, the compressive strength of concrete gets an increment of 8% and 25 at the 7th day and 2% and 4% at the 28th day, respectively. The further addition of sisal fiber reduces compressive strength. This is 8% and 12% at the 7th day and 4% and 5% decrease, respectively, as compared to 1% sisal fiber addition [30].

3.2.1. Split Tensile Strength. The splitting tensile strength test is an indirect tension test for concrete. It is carried out on a standard cylindrical specimen, tested on its side in diametric compression. In split tensile strength testing, the length of sisal fiber addition, namely, 10, 15, and 20 mm, was undertaken. Three cylindrical samples were tested for each length addition of sisal fiber. Then the average split tensile strength is recorded. Using 150 mm diameter and 300 mm height cylindrical samples, the split tensile strength of SFRC was studied at the AASTU laboratory. After the cylindrical split tensile strength samples were cured in water for 28 days, experimental tests were conducted according to ASTM C496. Accordingly, the addition of sodium hydroxide and sulfuric acid treated sisal fiber to concrete enhances split tensile strength up to a certain limit (P4 = 1.5%). The split tensile strength of the control mix after 28 curing days is 3.01 for the control mix, 3.21, 3.47, 3.62, and 3.83 MPa at an addition of sodium hydroxide and sulfuric acid treated sisal fiber of 0.5%, 1.00%, 1.25%, and 1.50%, respectively. This shows an increment of 6.6%, 15.2%, 20.2%, and 27.2% for P1, P2, P3, and P4 relative to the control mix. After the optimum limit, the split tensile strength tends to decrease when 1.75% and 2.00% of sodium hydroxide and sulfuric acid treated sisal fiber are added as compared to the control mix. The split tensile strength is 2.96 and 2.87 MPa at 1.75% and 2.00% fiber addition, respectively. This shows a 1.7% and 4.6% decrease.

Concrete is weak in tension. To support its weakness in tension, concrete is supplied by fiber. According to the study

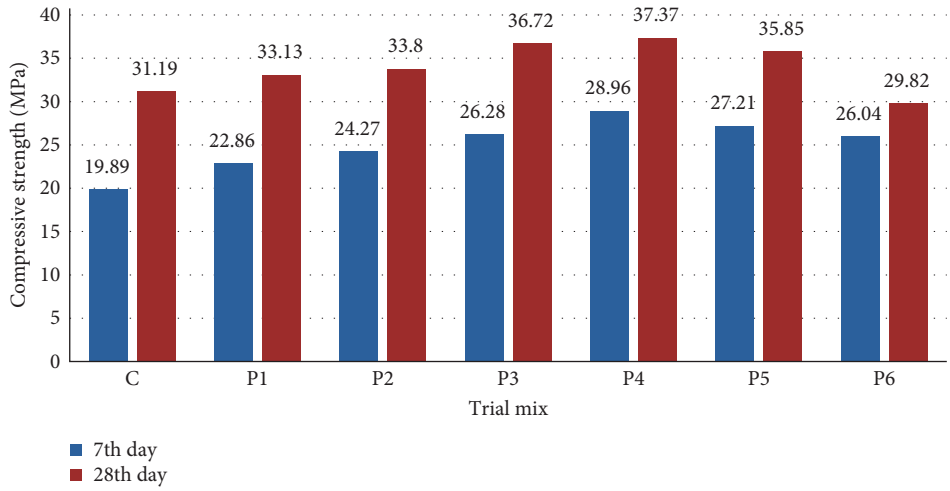

Figure 13: Mean compressive strength indicating the 7th and 28th curing days.

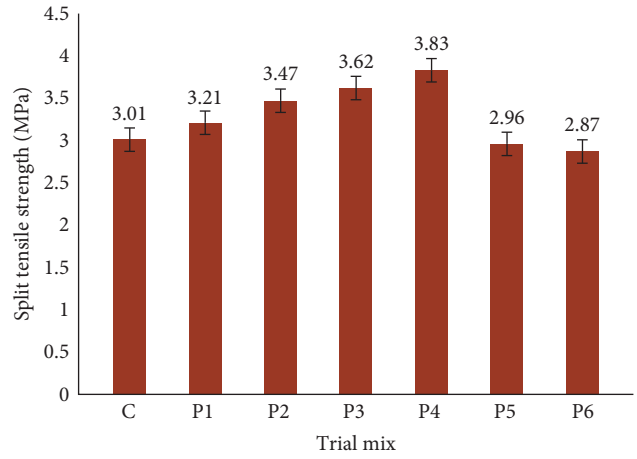

Figure 14: Split tensile strength at the 28th curing days.

[45], the addition of sisal fiber to the concrete matrix enhances the tensile property of concrete. In this study, the split tensile strength of 0.5%, 1%, and 1.5% sisal fiber shows an increment of 29% (2.2 MPa), 65% (2.8 MPa), and 106% (3.5 MPa) from the control mix (1.7 MPa). In this study, the split tensile strength shows a continuous split tensile strength enhancement as sisal fiber composition increases. In the work performed by Mithun et al. [30], using 0.5% and 1% fiber composition, 12% and 30% increments were observed at 7 days of curing. At the same curing days, 1.5% sisal fiber addition shows a decremental increase. This means that even if it shows enhanced tensile strength from the control mix, it is 13% lower than the split tensile strength achieved in 1% sisal fiber composition.

Further, when 2% sisal fiber composition was used, a 28% decrease was recorded as compared to the concrete with 1% sisal fiber. On the 28th curing day, the same trend was recorded. Six percent and 11% of split tensile strength were recorded at 0.5% and 1% sisal fiber composition as compared to the control mix. On the other side, 5% and 0.3% decrements were recorded when 1.5% and 2% sisal fiber were added to the concrete matrix, as compared to 1% sisal fiber composition. Laboratory results of shear strength are indicated in Figure 14.

Sher strength: For testing, shear strength of force was controlled to load with a rate of 2.5 K/s pace rates. V-notched shear samples were prepared at the AASTU laboratory to conduct a shear strength test. The shear load is applied at the center of a four-point adjusted Iosipescu shear test setup as shown in Figure 15 by adopting a uniform shear force distribution around the pure shear section. As performed according to ASTM D5379, the shear strength results of SFRC show an increment as compared to the control mix. Accordingly, at P1, P2, P3, and P4, the shear strength is recorded as 1.56, 2.02, 2.21, and 2.71 MPa, which is 23.8%, 60.3%, 75.4%, and 95.2%, respectively, as compared to the shear strength of the control mix (C = 1.26 MPa). However, P5 (1.75%) and P6 (2.00%) reduce the shear strength of the

Figure 15: Shear failure mode and cracking pattern.

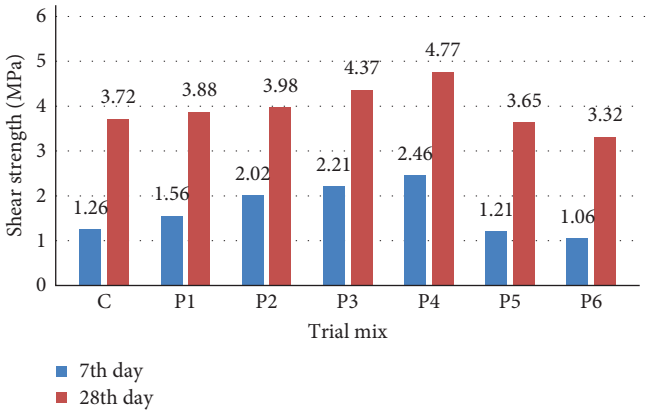

Figure 16: Shear strength of SFRC at the 7th and 28th curing days.

concrete to 1.21 and 1.06 MPa, respectively. This decrease indicates 3.9% at P5 ($P = 1.75\%$) and 15.8% at P6 (2.00%). Figure 15 is shear failure mode and cracking pattern of chemically treated sisal fiber-reinforced concrete.

Many researchers have been trying to study the shear strength of natural fibers using the V-notch (Iosipescu shear test) with the guidelines of ASTM standard D5379M [46]. From normal concrete (control mix), SFRC achieved higher shear strength with parallel trend lines. Accordingly, the shear strength of SFRC at 1% sisal fiber addition is 9.5% higher than that of normal concrete [47]. By testing M30 and M60 grades of concrete using sisal fiber as reinforcement, shear strength enhancement was observed. The shear strength of M30 at 0.5%, 1%, and 1.5% sisal fiber is 9.3, 10.0, and 11.17 MPa, which is 14%, 22%, and 37% higher than the control mix (8.17 MPa). For M30, the shear strength at sisal fiber compositions of 0.5%, 1%, and 1.5% is 6.5, 8.5, and 10.33, which indicates 18%, 55%, and 88% greater than the control mix. The results of shear strength are shown in Figure 16.

From this, it was observed that sisal fiber enhances the shear strength of concrete. This is because the addition of sisal fiber improves shear transfer within the concrete matrix by traversing over the voids available. Various studies have revealed the effectiveness of fiber-reinforced concrete in providing better shear strength and other mechanical properties. According to the study made by Oddo et al. [48], mechanical response and failure mode (shear strength) of concrete enhanced. This is due to adhesion properties achieved at the fiber-concrete matrix (interface).

3.3. Results of Microstructural Tests. SEM analysis can be used to examine the surface morphology of concrete, with concrete cube specimens tested using a benchtop SEM [19]. SEM analysis was performed at ASTU to reflect the internal image of hardened concrete of different fiber compositions with different resolution methods. SEM shows the interfacial image of concrete mix by revealing its C—S—H, CH, and pore structures. For microstructural SEM analysis, the control mix, the SFRC with improved compressive strength (P1, P2, P3, and P4), and P5 a total of six samples have been selected.

Figure 17 shows the SEM image of the control mix at different resolutions. Figure 18 labels the SEM images of P1 and P2 at different resolutions.

Figure 19 is the SEM image of P3 and P4, while Figure 6 is the SEM image of P5 at different resolutions. Pore structures, C—S—H crystals, C—H gel, and cracking patterns are shown in the same image with different appearances. In Figure 17, the pore structures are large, and the C—S—H crystal and C—H gel are shown in small amounts. On the other side, in Figure 19, the pore structures were reduced and the C—S—H crystal increased as compared to Figure 17.

Similarly, in Figure 17, the amount of pore structure reduces, and C—S—H crystal and C—H gel increase as compared to Figures 17, 18(a) and 18(b). In Figures 18 and 19, the chemically treated sisal fibers used in the concrete tend to be visible at a higher magnification level (×2,000). On the other hand, as shown in Figure 19, microcracks have been shown.

Accordingly, the morphological internal image of P3 (1.25%) and P4 (1.5%) is denser than the image of P1 (0.5%) and P2 (1.0%). Similarly, the SEM images of P1 and P2 are denser than C. From this, it is shown that, when the SEM image becomes denser, the pore structure reduces, while C—S—H crystals and C—H gel increase. Through the hydration reaction, the C—S—H crystals and C—H gel fill the microcracks and pore structures available in the concrete. This improves the durability and permeability of the concrete structure. The pore structures at 1.5% sisal fiber composition, as shown in Figure 19(b), are filled and crossed by

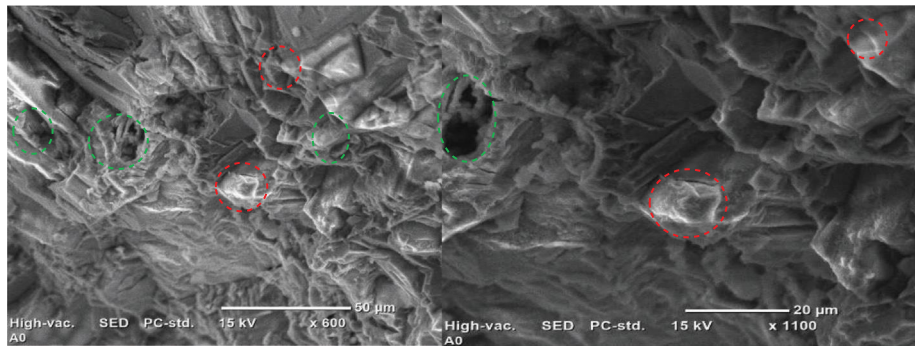

Figure 17: Microstructural image (SEM) of control mix magnified by different resolutions.

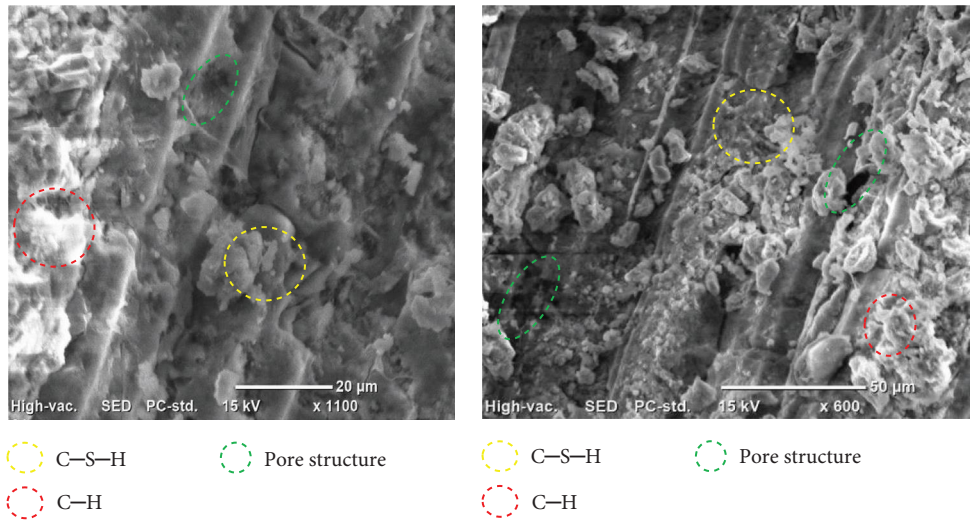

Figure 18: Microstructural image (SEM) (a) for P1 (0.5%) in a resolution of ×1,100 and (b) for P2 (1.00%) in a resolution of ×600.

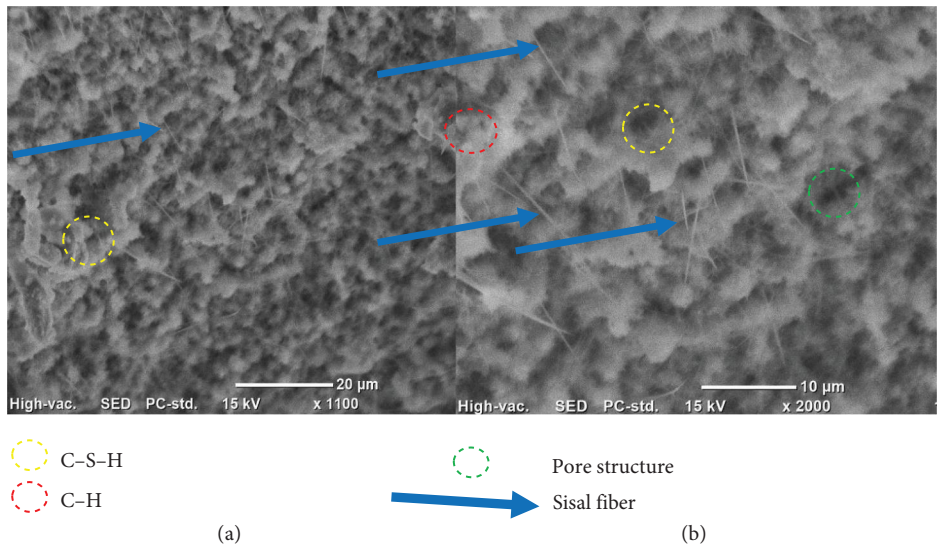

Figure 19: Microstructural image (SEM) (a) for P3 (01.25%) in a resolution of ×1,100 and (b) for P4 (1.5%) in a resolution of ×2,000.

the sisal fibers. This improves the shear resistance of the concrete. At P5 (1.75%), the creation of microcracks has been observed, and the amount of C—S—H crystals has reduced. This tends to decrease the quality of the concrete.

In line with the work of this paper, silica fume has a filler effect, as demonstrated by the work performed by Druta [49] on the title "Concrete Microstructure Characterization and Performance." The silica fume lowers porosity in the matrix and reduces internal bleeding while enhancing the matrix bond strength. This minimizes the growth of the production of calcium hydroxide in the interfacial transitional zone (ITZ) by maximizing the mechanical strength of the concrete.

According to the study made by Gelanew and Demiss [50], the incorporation of fiber showed a tight pore structure and well-formed interfaces when it incorporated limestone powder. The addition of fiber into concrete matrix particle size distribution influences SEM image of concrete. FRC shows that better macrostructure is due to the fineness of C—S—H particles as compared to conventional concrete. The crystalline phases are increased due to the addition of fiber in to concrete matrix.

X-ray diffraction (XRD): To identify the crystalline phase and mineralogical composition, an XRD test was made at ASTU. After a powder is prepared from the 28th day cured compressive strength sample, an XRD test was made in the same sample with SEM. The XRD results are shown on the x–y axis, where the x-axis represents degree (2θ) and the y-axis represents the intensity of the X-ray. Portlandite ($Ca(OH)^2$), calcium aluminum silicate (Al3CaO.5Si3O11), and silicon oxide (quartz) are the crystalline compositions observed during the XRD investigation. Every composition has its own function in the concrete matrix.

Portlandite, which is the mineral name of calcium hydroxide ($Ca(OH)^2$), contributes to the hydration reaction. Due to portlandite, cement reacts with water to give the concrete its strength.

This mineral composition, as shown in Figures 6–10, is presented in all the trial mixed concrete results, including the control mix. Quartz, the mineral name of silicon oxide (SiO_2), gets its name from sand and releases heat in the concrete matrix to activate the hydration reaction. C—S—H crystals are created when silica reacts with calcium during the hydration reaction of cement and water in the mixing process and long hydration action. Aluminum, calcium silicate, and calcium are also the other mineral compositions in the concrete matrix as a result of the XRD test results.

The XRD result for the control matrix is shown in Figure 7, for P1 (0.5%) is shown in Figure 7, for P2 (1.0%) is shown in Figure 8, and for P3 (1.25%) and P4 (1.5%) are shown in Figures 9 and 10, respectively. C—S—H crystals, the name for calcium silicate hydroxide, act as an additional binding agent in concrete matrix, because it generates binding agents when exposed to hydration reactions by dissolving in a C—H crystal. When calcium carbonate and aluminum silicates are combined, calcium aluminum silicate is created. In this XRD test result, calcium aluminum silicate was found in all the trial mixes, including the control mix.

At the control mix, the peak values were recorded at an intensity of 564, 490, 340, and 190 a.u. at an angle (2θ) of 34.9°, 26.5°, 18.2°, and 46.5° for portlandite, calcium silicate aluminum, calcium silicate hydrate, and quartz, respectively. Portlandite was produced due to the hydration reaction between CaO and $CaSiO_2$. From the cement as a composition, quartz or calcium hydroxide was found. For mix P1 (0.5%), the peak diffraction values were recorded at an intensity of 690, 540, and 290 at an angle (2θ) of 27.5°, 33.9°, and 23.5° for calcium aluminum silicate (CAS), portlandite, and quartz, respectively.

The peaks of CSH (calcium silicate hydrate) were recorded at an intensity of 600 and a peak angle of 29°. As compared to the control mix, P1 (0.5%) contains more CSH crystals. This implies the chemically treated sisal fiber gives the concrete mix a place to generate more CSH crystals. The generated CSH crystals provide a binding agent through the heat provided by calcium aluminum silicate and portlandite. The portlandite and the CAS on their sides release heat into the matrix by reacting with calcium oxide.

As shown in Figures 7–10, the peak composition value of CSH crystals increases as fiber content increases. This indicates that more CSH crystals generated in P1, P2, P3, and P4 (0.5%, 1.0%, 1.25%, and 1.5%) are due to the addition of chemically treated sisal fiber. At P4 (1.5%), the peak values were recorded as 1,150 a.u. at an angle of 18° and 610 a.u. at an angle of 27.5° for portlandite and CSH crystals, respectively. As indicated by the XRD results shown in Figures 7–10, the generation of portlandite and CSH crystals is in parallel. This helps to provide a ground for healthy hydration reactions in the concrete matrix.

According to the results of XRD, the CSH crystals recorded the highest in P4 as compared to P3, the highest in P3 as compared to P2, the highest in P2 as compared to P1, and the highest in P1 as compared to the control mix due to the addition of chemically treated sisal fiber. How could sisal fiber generate CSH crystals can be a question for the reader.

The chemicals sodium hydroxide and sulfuric acid were used to treat the sisal fiber to remove impurities present in the fiber. As the impurities were removed, a rough sisal fiber surface was provided. This improves the binding capability of the concrete ingredients. Coagulation of cement paste due to the presence of rough sisal fiber has been removed. The availability of portlandite led to the development of mechanical strength.

The presence of smaller portlandite contributes to the formation of C—S—H crystal, which fills the voids available in the concrete matrix through a long-term hydration reaction by forming C—H gel [51].

4. Conclusions

According to the experimental investigation on shear strength and microstructure of chemically treated sisal fiber, the following conclusions have been drawn.

Chemically treated sisal fiber addition enhances the mechanical properties of concrete. As compared to the control mix, an addition of 1.5% chemically treated sisal fiber

shows 46% and 20% compressive strength enhancement at the 7th and 28th days of curing as compared to the control mix. Twenty-seven percent enhancement was recorded in the split tensile strength of 1.5% SFRC as compared to the control mix at the 28th curing days. Shear strength of 1.5% SFRC was improved by 95% at the 7th curing days and 28% at 28th curing days as compared to the control mix. 1.5% SFRC shows denser SEM image as compared to the control mix. The cracking patterns have been improved in the SFRC as compared to the control mix. Moreover, more C—S—H crystals have been formed in the SFRC as compared to the control mix. In sum, the SEM image of chemically treated sisal fiber has been shown an improvement. Portlandite, quartz, calcium aluminum silicate, and C—S—H crystal were the common phases observed from the XRD result. Portlandite provides a ground for C—S—H crystal which contributes in creating binding and filler by dissolving the crystal in to C—H gel. From the total experimental investigation of compressive strength, split tensile strength, shear strength, and microstructure (SEM and XRD), the optimum amount of chemically treated sisal fiber to be added in to concrete for the formation of SFRC of enhanced property is 1.5%. Hence, 1.5% chemically treated sisal fiber shows improved mechanical and microstructural concrete properties.

Data Availability

Any main and/or supplementary data that have been used in the research is accessible to the correspondence email address.

Conflicts of Interest

The authors declare that they have no conflicts of interest.

Acknowledgments

This research is funded by Addis Ababa Science and Technology University.

References

[1] M. P. Iniya and K. Nirmalkumar, "A review on fiber reinforced concrete using sisal fiber," *IOP Conference Series: Materials Science and Engineering*, vol. 1055, no. 1, Article ID 012027, 2021.

[2] A. Punwar and J. R. Pitroda, "Study on insulated concrete forms using fibers: a review," *International Research Journal of Engineering and Technology (IRJET)*, vol. 9, no. 4, pp. 516–521, 2022.

[3] C. Palanisamy, N. Krishnaswami, S. K. Velusamy, H. Krishnamurthy, H. K. Velmurugan, and H. Udhayakumar, "Transparent concrete by using optical fibre," *Materials Today: Proceedings*, vol. 65, pp. 1774–1778, 2022.

[4] M. Shanmugamoorthy, S. Velusamy, A. Subbaiyyan, R. Yogeswaran, R. Krishnanbabu, and R. Senthilkumar, "Obtaining high durability strength using bacteria in light weight concrete," *Materials Today: Proceedings*, vol. 65, pp. 920–924, 2022.

[5] E. Mondo, *Shear capacity of steel fibre reinforced concrete beams without conventional shear reinforcement*, M.S. thesis, Royal Institute of Technology (KTH), Stockholm, Sweden, 2011.

[6] A. Varghese, R. K. Sajal, K. S. Sooraj, and K. D. Sanand, "Study of bond strength on various fibre reinforced concretes," *International Journal of Current Engineering and Scientific Research (IJCESR)*, vol. 5, no. 4, pp. 70–76, 2018.

[7] N. Kumar and A. Jaglan, "A review on use of fibers in concrete," *International Research Journal of Engineering and Technology (IRJET)*, pp. 549–551, 2020.

[8] W. A. Almatrudi, M. Alturki, O. M. Alawad, S. M. Alogla, and A. F. Elragi, "Effect of hybrid fibers on bond strength of fiber reinforced concrete," *ARPN Journal of Engineering and Applied Sciences*, vol. 15, no. 24, 2020.

[9] C. Druta, "Concrete microstructure characterization and performance," *Compressive Strength of Concrete*, vol. 90500, 2020.

[10] S. M. Dewi, M. N. Wijaya, and C. N. Remayanti, "The use of bamboo fiber in reinforced concrete beam to reduce crack," *AIP Conference Proceedings*, vol. 1887, no. 1, Article ID 020003, 2017.

[11] J. D. Dalvi, U. B. Kalwane, and P. Pasnur, "26 effect of fibre length and percentage of sisal on strength of concrete," *Multidisciplinary Journal of Research in Engineering and Technology*, vol. 3, no. 1, pp. 923–932, 2016.

[12] S. Shanmughan, S. Velusamy, J. L. Nallasamy et al., "Critical study on corrosion inhibitors in U-shaped RCC beams," *Advances in Materials Science and Engineering*, vol. 2022, Article ID 4762524, 8 pages, 2022.

[13] M. A. Aiello, F. Bencardino, A. Cascardi et al., "Masonry columns confined with fabric reinforced cementitious matrix (FRCM) systems: a round robin test," *Construction and Building Materials*, vol. 298, Article ID 123816, 2021.

[14] F. G. Carozzi, A. Bellini, T. D'Antino et al., "Experimental investigation of tensile and bond properties of carbon-FRCM composites for strengthening masonry elements," *Composites Part B: Engineering*, vol. 128, pp. 100–119, 2017.

[15] A. N. Rudresh and P. Shashank, "Experimental study on strength of fiber reinforced concrete for rigid pavements," *International Journal of Engineering Research & Technology*, vol. 5, pp. 2704–2710, 2018.

[16] S. Ragavendra, I. P. Reddy, and A. Dongre, "Fibre reinforced concrete—a case study," pp. 1–16, 2017, 33rd Natl. Conv. Archit. Eng. Natl. Semin. "Architectural Eng. Asp. Sustain. Build. Envel. ArchEn-BuildEn-2017, Hyderabad, India, no. December.

[17] N. Krishnaswami, S. Velusamy, C. Palanisamy, G. Prakash, K. K. Loganathan, and J. Moorthy, "Experimental studies on light weight concrete using gib & coconut shell in concrete," *Materials Today: Proceedings*, vol. 65, pp. 1307–1314, 2022.

[18] S. Velusamy, A. Subbaiyyan, K. Ramasamy et al., "Use of Municipal solid waste inert as a powerful replacement of fine aggregate in mortar cube," *Materials Today: Proceedings*, vol. 65, pp. 549–553, 2022.

[19] K. V. B. Krishnan, K. Nirmalkumar, V. Sampathkumar, and P. C. Murugan, "Experimental analysis of treated waste foundry and waste ceramics sand by replacement of fine aggregate in concrete," *Journal of Ceramic Processing Research*, vol. 24, no. 4, pp. 714–722, 2023.

[20] G. E. Arunkumar, K. Nirmalkumar, P. Loganathan, and V. Sampathkumar, "Concrete constructed with recycled water to experimental analysis of the physical behavior of polypropylene aggregate (PPA)," *Global NEST Journal*, vol. 25, no. 5, pp. 126–135, 2023.

[21] R. V. Yadav, R. Pratap, A. K. Pandey, S. N. Bajpai, S. Mishra, and A. Tiwari, "Case study on glass fibre reinforced concrete,"

International Research Journal of Engineering and Technology (IRJET), vol. 9, no. 3, pp. 7–10, 2022.

[22] A. Demissew, F. Fufa, and S. Assefa, "Partial replacement of cement by coffee husk ash for C-25 concrete production," *Journal of Civil Engineering, Science and Technology*, vol. 10, no. 1, pp. 12–21, 2019.

[23] M. Anas, M. Khan, H. Bilal, S. Jadoon, and M. N. Khan, "Fiber reinforced concrete: a review," *Engineering Proceedings*, vol. 22, no. 1, Article ID 3, 2022.

[24] K. Balasubramanian, "Current research and applications of fiber reinforced concrete composites in India," 2023.

[25] K. Joseph, K. Ghavami, and G. L. England, "The use of sisal fibre as reinforcement," *Construções Rurais e Ambiência*, vol. 3, no. 2, pp. 245–256, 1999.

[26] B. C. Thomas and Y. S. Jose, "A study on characteristics of sisal fiber and its performance in fiber reinforced concrete," *Materials Today: Proceedings*, vol. 51, pp. 1238–1242, 2022.

[27] I. O. Oladele, J. A. Omotoyinbo, and J. O. T. Adewara, "Investigating the effect of chemical treatment on the constituents and tensile properties of sisal fibre," *Journal of Minerals and Materials Characterization and Engineering*, vol. 9, no. 6, pp. 569–582, 2010.

[28] T. Mo, A. Shaikh, P. A. D. Raval, and J. R. Pitroda, "Experimental investigation on interlayer bonding strength of 3D printed concrete: a review," *International Research Journal of Engineering and Technology (IRJET)*, pp. 476–481, 2022.

[29] A. E. Bekele, H. G. Lemu, and M. G. Jiru, "Experimental study of physical, chemical and mechanical properties of enset and sisal fibers," *Polymer Testing*, vol. 106, Article ID 107453, 2022.

[30] K. Mithun, R. M. M. Gowda, and H. S. S. Chandra, "A study on structural characteristics of sisal fibre reinforced concrete," *International Journal of Engineering Research & Technology*, vol. 8, no. 6, pp. 1093–1096, 2019.

[31] Wijianto, R. M. D. Ibnu, and H. Adityarini, "Effect of NaOH concentration treatment on tensile strength, flexure strength and elasticity modulus of banana fiber reinforced polyester resin," *Materials Science Forum*, vol. 961, pp. 10–15, 2019.

[32] A. A. Allaie, "Partial replacement of fine aggregate with brick dust: a review," *International Journal of Technical Innovation in Modern Engineering*, vol. 5, pp. 3–7, 2019.

[33] I. G. Shaaban, A. H. Zaher, M. Said, W. Montaser, M. Ramadan, and G. N. A. Elhameed, "Effect of partial replacement of coarse aggregate by polystyrene balls on the shear behaviour of deep beams with web openings," *Case Studies in Construction Materials*, vol. 12, Article ID e00328, 2020.

[34] D. E. Ogheneochuko and O. U. Orie, "Optimization of superplasticized concrete using Taguchi approach: a case study of hydroplast 200," *Nigerian Journal of Technology*, vol. 37, no. 3, Article ID 611, 2018.

[35] K. G. Asfaw, "Investigation of the reasons for the unique growth and development of agave species (*Agave sisalana* and *Agave americana*) crop plants at the Southern, Central, North Western and Eastern parts of Tigray, Ethiopia," *Journal of Biological Sciences*, vol. 3, no. 4, pp. 273–281, 2011.

[36] T. P. Mohan and K. Kanny, "Chemical treatment of sisal fiber using alkali and clay method," *Composites Part A: Applied Science and Manufacturing*, vol. 43, no. 11, pp. 1989–1998, 2012.

[37] I. Shah, L. Jing, Z. M. Fei, Y. S. Yuan, M. U. Farooq, and N. Kanjana, "A review on chemical modification by using sodium hydroxide (NaOH) to investigate the mechanical properties of sisal, coir and hemp fiber reinforced concrete composites," *Journal of Natural Fibers*, vol. 19, no. 13, pp. 5133–5151, 2022.

[38] D. Yadav, G. R. Selokar, A. Agrawal, V. Mishra, and I. A. Khan, "Effect of concentration of NaOH treatment on mechanical properties of epoxy/sisal fiber composites," *IOP Conference Series: Materials Science and Engineering*, vol. 1017, no. 1, Article ID 012028, 2021.

[39] T. Yimer and A. Gebre, "Effect of fiber treatments on the mechanical properties of sisal fiber-reinforced concrete composites," *Advances in Civil Engineering*, vol. 2023, Article ID 2293857, 15 pages, 2023.

[40] J. Ritesh and M. Tech, "An interpretation on the properties of sisal fiber reinforced concrete with distinct proportions of fiber addition," *International Journal of Engineering Technologies and Management Research*, vol. 4, no. 3, pp. 469–475, 2017.

[41] Y. Negash, *Effect of enset fiber length on mechanical properties of concrete*, School of Civil and Environmental Engineering, 2021.

[42] P. K. Shah, M. K. Rana, and P. K. Kushwaha, "Experiments study on the strength properties of m30 concrete with glass fibers as a partial replacement for cement," *International Research Journal of Engineering and Technology (IRJET)*, vol. 9, no. 3, pp. 1475–1478, 2022.

[43] S. Acosta-Calderon, P. Gordillo-Silva, N. García-Troncoso, D. V. Bompa, and J. Flores-Rada, "Comparative evaluation of sisal and polypropylene fiber reinforced concrete properties," *Fibers*, vol. 10, no. 4, Article ID 31, 2022.

[44] M. B. Mekonen and G. W. Fayisa, "An investigation on effects of sisal fiber reinforced concrete on concrete properties," *Journal of Civil, Construction and Environmental Engineering*, vol. 7, no. 3, Article ID 23, 2022.

[45] M. A. Ali, "Strength and analysis of sisalfiber in concrete," pp. 2581–2589, 2020.

[46] F. Jauhar and H. S. Nasmi, "Shear properties evaluation of natural fibre reinforced epoxy composites using V-notch shear test Shear properties evaluation of natural fibre reinforced epoxy composites using V-notch shear test," *MATEC Web of Conferences*, vol. 195, Article ID 02004, 2018.

[47] F. O. P. Oriola, J. O. Afolayan, J. E. Sani, and Y. Adamu, "Estimating the shear strength of sisal fibre reinforced concrete," *Nigeria Journal ofTechnology*, vol. 38, no. 3, pp. 557–565, 2019.

[48] M. C. Oddo, G. Minafò, and L. La Mendola, "Experimental investigation on tensile and shear bond behaviour of Basalt-FRCM composites for strengthening calcarenite masonry elements," *Procedia Structural Integrity*, vol. 44, no. 2022, pp. 2294–2301, 2022.

[49] C. Druta, "Concrete microstructure characterization and performance," in *Compressive Strength of Concrete*, pp. 1–19, IntechOpen, 2019.

[50] D. M. Gelanew and B. A. Demiss, "Mechanical and microstructural properties of bamboo fiber-reinforced concrete containing a blend of waste marble powder and waste glass powder," *Advances in Civil Engineering*, vol. 2023, Article ID 2725801, 18 pages, 2023.

[51] A. U. Shettima, Y. Ahmad, M. W. Hussin et al., "Strength and microstructure of concrete with iron ore tailings as replacement for river sand," *E3S Web of Conferences*, vol. 34, Article ID 01003, 2018.